



1 Atmospheric nitrogen deposition to terrestrial ecosystems across 2 Germany

3 Martijn Schaap^{1,2}, Sabine Banzhaf², Thomas Scheuschner³, Markus Geupel⁴, Carlijn Hendriks¹,
4 Richard Kranenburg¹, Hans-Dieter Nagel³, Arjo J. Segers¹, Angela von Schlutow³, Roy Wichink
5 Kruit^{1,5}, Peter J. H. Builtjes^{1,2}

6 ¹TNO, Utrecht, The Netherlands

7 ²Free University Berlin, Institute of Meteorology, Germany

8 ³Ökodata, Berlin, Germany

9 ⁴UBA, Dessau, Germany

10 ⁵RIVM, Bilthoven, The Netherlands

11 *Correspondence to:* M. Schaap (martijn.schaap@tno.nl)

12

13 **Abstract.** Biodiversity is strongly affected by the deposition of nitrogen and sulfur on terrestrial ecosystems. In this paper
14 we present new quantitative estimates of the deposition of atmospheric nitrogen to ecosystems across Germany. The
15 methodology combines prognostic and empirical modelling to establish wet deposition fluxes and land use dependent dry
16 and occult deposition fluxes. On average, the nitrogen deposition in Germany was estimated to be 1057 eq ha⁻¹ yr⁻¹. The
17 deposition maps show considerable variability across the German territory with highest deposition on forest ecosystems in
18 or near the main agricultural and industrial areas. The accumulated deposition over Germany of this study is systematically
19 lower (27 %) than provided in earlier studies. The main reasons are an improved wet deposition estimation and the
20 consolidation of improved process descriptions in the LOTOS-EUROS chemistry transport model. The presented
21 deposition estimates show a better agreement with results obtained by integrated monitoring and deposition modelling by
22 EMEP than the earlier results. Through comparison of the new deposition distributions with critical load maps it is estimated
23 that 70% of the ecosystems in Germany receive too much nitrogen.

24

25 1 Introduction

26 Anthropogenic activities generate a tenfold more reactive nitrogen (Nr) than in the late 19th century due to increased
27 agricultural production and energy consumption (Galloway et al., 2003). Globally half of the annually fixed nitrogen is due
28 to anthropogenic activities (Fowler et al., 2013). A large part of the reactive nitrogen enters the atmosphere in the form of
29 ammonia (NH₃) through animal husbandry and fertilizer use as well as in the form of nitrogen oxides (NO_x) through
30 combustion of fossil fuels (Erisman et al., 2011). The remainder is released as nitrous oxide (N₂O) or as nitrate (NO₃) to
31 the soil-water compartment. In Germany about 26 % of total Nr is emitted as NO_x and about 30 % as NH₃ (Geupel and
32 Frommer, 2015). Deposition of reactive nitrogen has negative impacts on biodiversity and ecosystem functioning (Sutton
33 et al., 2011). Especially in ecosystems adapted to nutrient poor conditions, a long term and sizeable input of reactive
34 nitrogen may negatively affect plant communities (Bobbink et al., 1998). Field studies have shown an inverse relationship
35 between reactive nitrogen deposition and species diversity (Damgaard et al., 2011). To assess the extent to which an
36 ecosystem is at risk the critical load concept has been developed (Hettelingh et al., 1995). Currently, it is estimated that
37 about half of the European ecosystems receive nitrogen in excess to the critical load (Hettelingh et al., 2013).



38 Major sources of oxidized nitrogen in western Europe are road transport, electricity generation, and shipping (Kuenen et
39 al., 2014). Nitrogen oxides play a key role in atmospheric chemistry (Crutzen, 1979). Only a fraction is removed from the
40 atmosphere close to their sources as the nitrogen oxides need to be further oxidized before they are effectively deposited
41 (Hertel et al., 2012). Reduced nitrogen emissions in the form of ammonia are mostly associated with agriculture, though
42 other minor sources play a role (Bouwman et al., 1997). Ammonia is emitted during and after application of fertilizer to the
43 land, from senescence of plants, animal excretion in housing systems, during grazing and after application of manure, in food
44 processing and fertilizer production, and as a byproduct from car exhaust equipped with a three-way catalyst (Erisman et
45 al., 2007; Galloway et al., 2003). The atmospheric lifetime of ammonia is limited to several hours as it is effectively
46 removed by dry and wet deposition and it readily reacts with sulfuric and nitric acid to form particulate ammonium salts
47 (Fowler et al., 2009). In contrast to oxidized nitrogen a large proportion of reduced nitrogen is deposited relatively close to
48 its source. Through the formation of ammonium nitrate the atmospheric cycling of reduced and oxidized nitrogen are
49 connected (Erisman and Schaap, 2004). The particulate salts have a longer atmospheric life time providing a means of long
50 range transport of reactive nitrogen (Hertel et al., 2012). Assessments of the exposure of sensitive ecosystems and
51 consequent development of mitigation strategies need to take into account the different behavior among the nitrogen
52 compounds.

53 The development of European mitigation strategies to reduce ecosystem exposure within the UNECE-CLRTD convention
54 is supported by atmospheric modelling using the EMEP model (Simpson et al., 2012). This modelling system is a consensus
55 model applied to the full European domain with a coarse resolution. In the nineties the EMEP model was used on a 125
56 Km resolution, which was increased to 56 Km and currently 28 Km. In Germany, and most other countries, it was
57 recognized that this resolution does not provide sufficient detail for national assessments. Moreover, establishing the
58 deposition distributions based on modelling alone is challenging. The nitrogen cycle is complex and chemistry transport
59 models may show significant biases against observations (Vautard et al., 2006). One of the causes of the biases is related
60 to the precipitation information commonly used in chemistry transport models, which is often not very accurate and does
61 not reflect small scale variability due to orographic effects resulting in relatively poor representation of the gradients in the
62 wet deposition flux (Simpson et al., 2006). Hence, whereas there is no alternative for modelling to establish the dry
63 deposition, empirical approaches are often favoured for the mapping of wet deposition fluxes. A large number of monitoring
64 sites providing precipitation chemistry exist in national and European networks (Tørseth et al., 2012; Waldner et al., 2014).
65 In many studies wet deposition distributions are obtained through an interpolation of rain water composition and subsequent
66 multiplication with precipitation maps (Rihm and Kurz, 2001). Finally, a specific challenge concerns the assessment of the
67 occult deposition, which may contribute considerable inputs to ecosystems at higher altitudes (Blackwell and Driscoll,
68 2015). We aim to quantify the critical load exceedance for nitrogen across Germany based on a national scale mapping
69 procedure for the individual deposition pathways.

70 In this study we present the methodology for the assessment of the nitrogen deposition across Germany and illustrate it
71 with results for 2009. The methodologies to assess the wet, dry and occult deposition are presented in chapter 2. The
72 resulting new deposition estimates as well as critical load exceedances are presented and discussed in section 3. We
73 summarize the main findings of the study in section 4.

74



75 2 Methodology

76 2.1 Overall approach

77 To estimate the nitrogen deposition to ecosystems across the German territory as good as possible a complex procedure is
78 followed. For pragmatic and historical reasons the assessment strategy combines empirical procedures with chemistry
79 transport modelling results. A short overview is presented in this subsection while a more detailed description of the
80 calculation of the different deposition pathways is given in the following subsections. Figure 1 provides an overview of this
81 procedure including the most important input and intermediate data sets as well as data flows. As there is no large dataset
82 of dry deposition observations we rely on chemistry transport modelling to assess the land use specific dry deposition
83 distributions across Germany. The LOTOS-EUROS CTM is used to model the dry deposition distributions at $7 \times 7 \text{ km}^2$
84 across Germany. Long range transport is incorporated by nesting the German study area into a simulation over Europe as
85 a whole. Besides the deposition fluxes also the modelled rain water concentrations are used in the next steps of the
86 deposition assessment. As the monitoring of wet deposition is rather straightforward, a few hundred stations provide
87 precipitation chemistry in Germany. The density of the observations allow to perform an empirical assessment of the wet
88 deposition flux. These data are used to correct the LOTOS-EUROS rain water concentration distribution towards the
89 observed data using residual kriging. The resulting rain water distribution is combined with a high resolution precipitation
90 distribution to arrive at the final wet deposition estimates. In this way a highly resolved map based on empirical data is
91 obtained that benefits from the process knowledge incorporated in the LOTOS-EUROS model.

92 Currently, none of the European Eulerian chemistry transport models incorporates a parameterization of the occult
93 deposition. For countries with only small areas of upland, this will not lead to significant underestimates in total deposition.
94 However, for elevated locations it may be a substantial contribution to total deposition. In this study the occult deposition
95 flux is derived by estimating the deposition flux of cloud and fog water which is combined with the pollutant concentration
96 in the cloud water. The cloud water concentrations are deduced from the rain water concentrations. The challenge to
97 estimate the occult deposition is to capture the variability in the cloud deposition flux which is strongly dependent on
98 altitude, slopes and local meteorology. Therefore we use high resolution meteorological data available for Germany as a
99 whole, i.e. $7 \times 7 \text{ km}$. Note that this resolution is not able to capture high resolution variability, which means that the occult
100 deposition reflects background values for larger regions and do not reflect the deposition at very exposed sites.

101 To arrive at the final result the distributions of dry, wet and occult deposition fluxes are simply added. This addition takes
102 place on the high resolution grid of the precipitation ($1 \times 1 \text{ km}^2$). Note that although the fluxes are provided on this high
103 resolution the underlying fluxes are not all resolved on this resolution.

104 2.2 Chemistry transport modelling

105 To assess the land use specific dry deposition distributions across Germany we used the 3-D regional chemistry transport
106 model LOTOS-EUROS (Schaap et al., 2008), which is aimed at the simulation of air pollution in the lower troposphere.
107 The model is of intermediate complexity in the sense that the relevant processes are parameterized in such a way that the
108 computational demands are modest enabling hour-by-hour calculations over extended periods of several years within
109 acceptable computational time. The model is a so-called eulerian grid model, which means that the calculations for
110 advection, vertical mixing, chemical transformations and removal by wet and dry deposition are performed on a three



111 dimensional grid. The LOTOS-EUROS model has a long history studying the atmospheric nitrogen and sulphur cycles.
112 Many scientific studies have been carried out with the LOTOS-EUROS model studying secondary inorganic aerosol
113 (Banzhaf et al., 2015; Erisman and Schaap, 2004; Schaap et al., 2004, 2011), sea salt (Manders et al., 2010), particulate
114 matter (Hendriks et al., 2013; Manders et al., 2009), ozone (Beltman et al., 2013; Curier et al., 2012), nitrogen dioxide
115 (Curier et al., 2014; Schaap et al., 2013) and ammonia (Hendriks et al., 2016; Van Damme et al., 2014; Wichink Kruit et
116 al., 2012). For details on the model we refer to these publications.

117 Here we outline the main features of the LOTOS-EUROS version 1.10 used in this study. The partitioning between the gas
118 and aerosol phase for ammonia/ammonium and nitric acid/nitrate is treated by ISORROPIA2 (Fountoukis and Nenes,
119 2007). Reaction of nitric acid with sea salt to form coarse sodium nitrate is included in a dynamical way. This model version
120 also includes a pH dependent cloud chemistry scheme (Banzhaf et al., 2012). The scheme for in- and below-cloud
121 scavenging of gases and particles accounts for droplet saturation (Banzhaf et al., 2012). The LOTOS-EUROS model is one
122 of the few chemistry transport models that uses a description of the bi-directional surface-atmosphere exchange of NH_3
123 (Wichink Kruit et al., 2012). The surface-atmosphere exchange module DEPAC is used for modelling the dry deposition
124 of gases (Van Zanten et al., 2010). The module in LOTOS-EUROS was expanded to include the co-deposition effect of
125 sulphur dioxide and ammonia. The deposition of particles is represented adapting the methodology of Zhang et al. (2001).
126 For a detailed analysis of the impact of including these process descriptions into LOTOS-EUROS we refer to a dedicated
127 sensitivity study (Banzhaf et al., 2016).

128 The LOTOS-EUROS model was ran for the year 2009 using ECMWF meteorological data to drive the model. Through a
129 one-way nesting procedure a simulation over Germany was performed on a resolution of 0.125° longitude by 0.0625°
130 latitude, approximately 7 by 7 km^2 . The high resolution domain is nested in a European domain with a resolution of 0.5°
131 longitude by 0.25° latitude, approximately 28 by 28 km^2 . The emissions that were fed into the LOTOS-EUROS model were
132 different for the two modelling domains. For the European background simulation the TNO MACC-II European emission
133 inventory for the year 2009 (Kuenen et al., 2014) was used. For the nest the emission data for Germany were replaced by
134 national data. The available national data contain sector specific emissions for the year 2005 on a regular grid with a
135 resolution of $1/60^\circ$ longitude by $1/60^\circ$ latitude (about $1.2 \times 1.9 \text{ km}^2$). This emission inventory has been produced by the
136 Institut für Zukunftsstudien und Technologiebewertung (IZT) and the University of Stuttgart within the PAREST project
137 (Jörß et al., 2010). This is the most up-to-date spatially distributed inventory for Germany as a whole. Note that the emission
138 data were produced on county basis and that land use information was used to disaggregate the emission information to a
139 higher resolution. This means that the detail in the emission grids is limited, explaining why the modelling was not
140 performed at higher resolutions than $7 \times 7 \text{ km}$. To account for the emission situation in 2009 the PAREST emissions for
141 Germany were scaled on a sector basis to the officially reported emission totals for 2009 as reported in 2014 by
142 UNECE/CLRTAP (www.uba.de). The temporal variation of the emissions is represented by monthly, day-of-the-week and
143 hourly time factors that break down the annual totals for each source category (Schaap et al., 2004).

144 For evaluation purposes we use data from the national database maintained by UBA. This database includes data for sulphur
145 dioxide (N=31) and nitrogen dioxide (N=45) at rural background locations. For ammonia only very few data are available
146 within this database. Hence, we have conducted an effort to collect ammonia measurements from passive samplers networks
147 operated by different institutions across the country. For 6 networks stations with data were obtained for the years 2009-
148 2011. Most networks provided data for 2010 and 2011, leaving 2009 less covered. Hence, we have averaged the
149 concentrations over the 2009-2011 period to compare to our modelled ammonia distribution. Five stations with



150 concentrations far above $7 \mu\text{g}/\text{m}^3$ were removed from the analysis as they were considered hot spot locations. The modelled
151 wet deposition fluxes were compared to observed values as presented below.

152 2.3 Wet deposition estimation

153 Traditionally, the assessment of wet deposition fluxes to ecosystems in Germany is performed with an empirical approach
154 making use of observed wet deposition fluxes at a large number of stations (Bultjes et al., 2011; Gauger et al., 2008). In
155 this study we derive rain water concentrations at the measurement locations and interpolate these data across Germany to
156 arrive at a nationwide distribution. The distribution of the concentration in rain water is then multiplied with a high
157 resolution precipitation map to arrive at the wet deposition estimates:

$$158 \quad F_{\text{wet}} = C_{\text{rainwater}} * \textit{Precipitation amount} \quad (\text{Equation 1})$$

159 Datasets on precipitation chemistry from various national and regional monitoring programs in Germany were compiled
160 providing information for 260 sites. The national UBA network (n=11) samples on a weekly rhythm, whereas the regional
161 networks (n=249) may operate at a weekly, two-weekly, four-weekly or monthly basis. Unfortunately, the sampling
162 strategies of the regional networks are not synchronised, only allowing an assessment on annual average basis. The majority
163 of the wet deposition data is obtained with bulk samplers as only 40 stations are equipped with wet-only samplers. Hence,
164 the data from the bulk samplers that pass our quality control procedures were corrected for the dry deposition into the
165 funnels using species dependent correction factors (Gauger et al., 2008). As the wet deposition data are obtained from many
166 different sources a common quality assessment and quality control (QAQC) protocol and data selection procedure was
167 applied to the whole database. Following EMEP protocols (EMEP, 1996) the ion balance is calculated for all samples. In
168 case the net ion-charge exceeds $\pm 20\%$, the measurement is rejected. To remove further outliers a statistical outlier test is
169 performed for the time series of each station using the Grubbs test (Grubbs, 1969). The procedure is iterative in the sense
170 that the procedure is repeated after identifying and removing an outlier until no outliers are found anymore, or too many
171 entries from the series are removed. As we log-transform the data in the interpolation scheme, the procedure is applied to
172 the time series of log-concentrations. All in all, most data flagged invalid are largely due to the ion balance check.

173 A minimum valid data coverage of 40% for a given year was required to be included in further analyses. This criterion is a
174 compromise between including as many stations as possible and maintaining high data quality. The 40% criterion was
175 established based on a pragmatic approach in which we averaged the concentration in precipitation measured at UBA
176 stations for 1000 random subsets of the available 52 weekly measurements for different data availabilities, i.e. 100%, 80%,
177 60%, 40% and 20%. As expected, the variability around the annual mean increases when data availability becomes smaller.
178 At 40% availability the standard deviation is around 15% of the mean concentration values for sulfate, nitrate and
179 ammonium, which we feel is in line with uncertainties in precipitation amounts and other concentration data.

180 Within this study we used a residual kriging methodology to generate the rain water concentration distribution across
181 Germany for 2009 (Wichink Kruit et al., 2014). Within this procedure the difference between the residual between the
182 observations and an a priori distribution is interpolated. The a priori distribution is the modelled average rain water
183 concentration from the LOTOS-EUROS model. The advantage of using LOTOS-EUROS distributions as a priori is that
184 we use process knowledge in the interpolation, which results in better validation statistics (Wichink Kruit et al., 2014). As
185 there is considerable variability between observed concentrations at stations at distances close to each other there remains
186 a residual between the observed and optimized distribution. Evaluations of the interpolated fields with the measured data



187 shows that for ammonium the differences can be as large as 25%, whereas the differences for nitrate and sulfate are much
 188 smaller (~10%). This can be explained by the much smaller gradients across Germany observed in the rain water
 189 concentrations for nitrate and sulfate compared to those for ammonium.

190 Finally, the rain water concentration is multiplied by a high resolution precipitation map for Germany (see Figure 2). This
 191 map is derived from precipitation measurements by the German Weather Service using geostatistical approach with a linear
 192 regression between precipitation and elevation (Herzog and Muller-Westermeier, 1998). A mean error of 8% was estimated
 193 for the annual precipitation amounts by (Herzog and Muller-Westermeier, 1998). We validated this distribution against the
 194 independent information on precipitation amounts from the stations with precipitation chemistry. Overall, the comparison
 195 is very good with most annual totals within 15% of each other. The higher inaccuracy reported here could well be associated
 196 to the host of different samplers and the sometimes long sampling periods (up to one month) used within the wet deposition
 197 networks. Field inter-comparison of different bulk and wet-only samplers has found it difficult to estimate precipitation
 198 volumes accurately. For instance, an accuracy better than 10% was only reached for 10–20% of the individual samples
 199 during a comparison held in the Netherlands with samplers from 20 different countries (Erisman et al., 2003).

200 2.4 Occult deposition estimation

201 The occult deposition computed within this work refers to nitrogen input by orographic clouds, which is the result of
 202 condensation processes in moist air lifted by mountains. Generally, the occult flux F_{occult} is derived by the multiplication of
 203 the deposition flux of fog water F_{Fog} and the pollutant concentration in the fog water C_{Fog} :

$$204 \quad F_{occult} = F_{fog} * C_{fog} \quad \text{(Equation 2)}$$

205 The calculation of fog water deposition (F_{Fog}) follows the approach by (Katata et al., 2008, 2011). In Katata et al. (2008) a
 206 simple linear equation for the fog deposition velocity v_d based only on horizontal wind speed has been derived from
 207 numerical experiments using a detailed multilayer land surface model that includes fog deposition onto vegetation
 208 (SOLVEG):

$$209 \quad v_d = A * U \quad \text{(Equation 3)}$$

210 where A is the slope of v_d that depends on vegetation characteristics (nondimensional), and U the horizontal wind speed
 211 [$m\ s^{-1}$] above the canopy. A is calculated by:

$$212 \quad A = 0.0164 * \left(\frac{LAI}{h}\right)^{-0.5} \quad \text{(Equation 4)}$$

213 where LAI is the Leaf Area Index and h the canopy height [m]. The calculations of A using Equation 4 agreed with
 214 observations in various cloud forests with $LAI/h > 0.2$ (Katata et al., 2008) and it was stated that Equation 4 can be widely
 215 used to predict cloud water deposition on forests with $LAI/h > 0.2$. Using v_d the flux of fog water deposition F_{Fog} [$kg\ m^{-2}\ s^{-1}$]
 216 is calculated using:

$$217 \quad F_{Fog} = v_d * \rho * q_c = A * u * \rho * q_c \quad \text{(Equation 5)}$$

218 where ρ is the air density [$kg\ m^{-3}$], u and q_c are the horizontal wind speed [$m\ s^{-1}$] and the liquid water content [$kg\ water\ kg$
 219 air^{-1}] near the surface, respectively. The accuracy of Equation 5 in the amount of fog deposition has been validated with



220 data on turbulent fog flux over a coniferous forest in Germany (Klemm and Wrzesinsky, 2007) with a prediction error of
221 13% (Katata et al., 2011).

222 The meteorological input to calculate the occult deposition flux was taken from the COSMO-EU model which is the
223 operational NWP model of the German Weather Service (DWD). COSMO-EU was chosen as it provides the meteorological
224 fields over Germany on a rather high grid resolution of ca. $7 \times 7 \text{ km}^2$. Hourly data of the meteorological fields were used to
225 calculate the annual fog water deposition flux based on Equation 5 with

$$226 \quad F_{Fog(annual)} = \sum_t v_d(t) * \rho(t) * q_c(t) = A * \sum_t u(t) * \rho(t) * q_c(t) \quad (\text{Equation 6})$$

227 where ρ is the air density [kg m^{-3}], q_c is the liquid water content [$\text{kg water kg air}^{-1}$] at the lowest atmospheric model layer
228 and u the horizontal wind speed at 10 m [m s^{-1}]. The elevation of u may be different from that of U in Equation 3 in some
229 cases, but this does not cause a significant error in representative wind speed according to the logarithmic wind profile in
230 the surface boundary layer (Katata et al., 2011).

231 The approach following Katata (2008;2011) as described above is based on experimental data in forests and hence, provides
232 an estimation of fog water deposition on forests only. Furthermore, the input on vegetation by fog is much more relevant
233 for forests than for other land use categories as e.g. for grassland as the area of incidence is largest for forests when they
234 filter the air mass passing through including fog or clouds. Hence, available studies on the occult input on vegetation are
235 limited on forests and therefore fog water deposition on land use categories other than forest categories are neglected here.

236 The mean pollutant concentration in fog water (C_{Fog}) was estimated from the annual mean concentration in rainwater using
237 so called enrichment factors (=EF):

$$238 \quad C_{Cloud} = C_{Rain} * EF \quad (\text{Equation 7})$$

239 Hereby the annual mean concentrations in rainwater per species stem from the interpolated concentration fields derived for
240 the calculation of the wet deposition flux. The enrichment factors for the different species were derived from a compilation
241 of field data from studies that provide simultaneous observations of fog and rain water chemistry (Table 1). The
242 underpinning studies are provided in the supplementary material. Enrichment factors are greater than unity for all species
243 as within all available studies and for all species the concentration in fog water was higher than in rain water. This can be
244 explained by a lower dilution in fog/cloud droplets as these are smaller than rain droplets and contain less water. The
245 variability between the individual studies is large indicating the enrichment factors may be a large source of uncertainty.

246

247

248 **3 Results and discussion**

249 **3.1 Deposition fluxes**

250 The estimated average deposition fluxes for Germany in 2009 are summarized in **Error! Reference source not found.**
251 The estimated total deposition of reactive nitrogen amounts to $1057 \text{ eq ha}^{-1} \text{ a}^{-1}$ on average across the country. Almost two
252 thirds (64%) of the nitrogen deposition is explained by reduced nitrogen, whereas oxidised nitrogen contributes the rest
253 (34%). The deposition of oxidized and reduced nitrogen show distinct patterns across the country (See Figure 3). Deposition
254 of reduced nitrogen maximises in the north west and in the south east of the country, basically mirroring the distribution of



255 animal density in Germany. For reduced nitrogen, the estimated fluxes indicate that the contributions of dry ($337 \text{ eq ha}^{-1} \text{ a}^{-1}$)
256 ¹) and wet ($327 \text{ eq ha}^{-1} \text{ a}^{-1}$) deposition are almost equal on average. However, the relative contributions show considerable
257 variability as in source areas for ammonia the dry deposition dominates. In more natural regions the wet deposition is about
258 two times more important than the dry flux. For oxidized nitrogen the deposition is highest in the Ruhr area. In addition, a
259 number of other large agglomerations can be recognized, such as Frankfurt, Stuttgart, and Berlin. As opposed to reduced
260 nitrogen, the wet deposition ($248 \text{ eq ha}^{-1} \text{ a}^{-1}$) is more important than the dry deposition ($131 \text{ eq ha}^{-1} \text{ a}^{-1}$) as the dry deposition
261 velocities of NO_x are relatively small compared to those of ammonia. The oxidation of nitrogen oxides to nitric acid and
262 subsequent formation of particulate ammonium nitrate, especially during winter and spring, favours the long range transport
263 and removal through precipitation. Wet deposition fluxes for both components show (secondary) maxima in areas with
264 high precipitation amounts, i.e. mountainous areas like the alpine region, the Black Forest, the Erz Mountains and the Harz
265 Mountains. The calculated contribution of occult deposition is generally negligible at low altitudes but becomes only
266 important in the mentioned mountainous regions. Surprisingly, the occult deposition in the black forest is estimated to be
267 quite low, which is associated with relatively low values of liquid water content near the surface within the COSMO-EU
268 model during 2009.

269 The dry deposition flux is strongly dependent on land use category through surface roughness and substance properties
270 such as solubility or reactivity. In Table 2 the land use dependent dry deposition is listed. The comparison between land
271 use classes clearly illustrates that the higher roughness of the forest classes cause increased dry deposition compared to low
272 vegetation classes such as grasslands. The average fluxes for inland surface waters and forests are about a factor 2.5 apart.

273 Due to the combination of empirical results for the wet and occult deposition and modelling results for the dry deposition
274 it is important to assess the quality of the dry deposition estimates. This can only be done indirectly as observations for dry
275 deposition are hardly available. Of special interest is the consistency between the modelled and observed wet deposition
276 fluxes. Below, we discuss the evaluation of the LOTOS-EUROS model results in more detail.

277

278 3.2 Evaluation of the chemistry transport modelling

279 3.2.1 Evaluation of modelled concentrations

280 In Figure 5 the comparison of the modelled and observed annual average concentrations are shown. The model tends to
281 underestimate the observed NO₂ concentrations by on average 22%. For NO₂ there are many stations that show a close
282 correspondence to observed values near the one-to-one line. However, there are also a number of stations for which the
283 modelled values are about $2\text{--}4 \mu\text{g m}^{-3}$ lower than those observed. Overall the gradient of NO₂ over the country is addressed
284 well. For SO₂ the same conclusion can be drawn, albeit that on average a small overestimation is observed. As the modelling
285 of all the processes including deposition occurs on an hourly time resolution it is interesting to see if the model reproduced
286 the seasonality and variability on observation stations. Therefore, in Figure 6 examples for the time series comparison are
287 shown for two stations in Germany. It can be observed that the model captures the seasonal variability in both components.
288 Moreover, on a short time scale many of the episodes with high concentrations are captured. Similar findings have been
289 reported focussing on total atmospheric NO₂ columns in the Netherlands (Vlemmix et al., 2015). The major episode of
290 nitrogen dioxide in January is captured less well which may be due to very stable conditions in parts of Germany. As the



291 exact timing of the plumes is often off by a few hours we calculated the temporal correlation coefficient on the basis of
292 daily averages. The correlation coefficients (r^2) are very reasonable with values of 0.71 for NO_2 and 0.59 for SO_2 (see
293 Table 3). In short, we feel that the distributions of nitrogen dioxide and sulphur dioxide on rural background stations is
294 simulated satisfactorily.

295 Figure 5c shows the evaluation results for annual mean ammonia concentrations. On average, the model tends to
296 underestimate the observed concentrations slightly and yields an explained spatial variability of 65%. Hence, the model is
297 able to reproduce a large part of the variability and large scale gradients across Germany. Within a given region, e.g. Lower
298 Saxony, still considerable spread around the 1:1 line is observed, which we attribute to the low level of spatial detail in the
299 emission inventory within counties. Overall, the model performance for a regional assessment is promising. In a next step
300 is seems logical to also investigate the seasonal cycles and search for high resolution data sets. As ammonia levels are
301 highly variable more detailed emission information is anticipated to improve the comparison further.

302

303 3.2.2 Dry deposition velocity

304 In Table 4 the average and effective dry deposition velocities to land use classes are tabulated. The effective dry deposition
305 velocities defined as the annual average flux divided by the annual mean concentration are usually lower than those of the
306 average velocity. This is due to the anti-correlation between the dry deposition velocity and the atmospheric concentration
307 of most pollutants. For example, NO_2 concentrations show a day time and summer minimum, whereas the dry deposition
308 velocity maximizes at these times. Hence, the annual effective dry deposition velocity is lower than the mean of the hourly
309 velocities. The only exception is nitric acid because its concentration (day time and summer maximum) correlates strongly
310 with the dry deposition velocity leading to a higher effective than average dry deposition velocity. The distribution of the
311 annual mean and effective deposition velocities (at 2.5 m) show little variation across Germany although the seasonal
312 variability in the more continental south is larger than in the north. The deposition velocity of ammonia behaves differently
313 as it includes the impact of the compensation point. Figure 7a clearly illustrates the inverse relationship between the
314 concentration level and the effective dry deposition velocity for coniferous forest for ammonia (left panel). In the large
315 forest areas in Germany velocities up to 2 cm/s are modelled, whereas in ammonia rich areas in Lower Saxony and Bavaria
316 values below 1 cm/s are modelled. The lower dry deposition velocity in the ammonia source areas is a direct consequence
317 of the compensation point approach included in the dry deposition module. In Figure 7b we compare the range of modelled
318 annual mean dry deposition velocities across Germany to a compilation of values reported in literature (Schrader and
319 Brümmer, 2014). Note that this comparison should be considered as indicative as the literature data have been obtained by
320 a host of different methodologies spanning different climatic conditions. Moreover, the modelled deposition velocities refer
321 to 2.5 m height, whereas the literature data often do not specify the representative height. Still, we conclude that the range
322 of the modelled dry deposition velocities for ammonia is plausible and that there are no indications that the modelled values
323 are unrealistic.

324



325 3.2.3 Wet deposition

326 For the evaluation of the wet deposition fluxes of LOTOS-EUROS we compare to the data of 150 stations used for the
327 empirical assessment of the wet deposition flux. The model underestimates the wet fluxes for all components. The
328 underestimation is lowest for reduced nitrogen (21%), see Table 5. Oxidized nitrogen shows an underestimations of 38%.
329 In absolute terms the underestimation is about $140 \text{ eq ha}^{-1} \text{ yr}^{-1}$ for reactive nitrogen. In comparison to the observations the
330 variability of the modelled wet deposition fluxes is rather small. Although models always tend to underestimate observed
331 variability, we feel that one of the main reasons for lower variability is high spatial and temporal variability in precipitation
332 amounts and the general challenge for meteorological models to realistically represent these variabilities. This hypothesis
333 was tested by combining the empirically derived high resolution precipitation map and the modelled rain water
334 concentrations. This exercise showed a considerable improvement for the spatial correlation between the calculated wet
335 deposition fluxes. and station observations, confirming the hypothesis. It should be noted that, as expected, the exercise did
336 not affect the bias.

337

338 3.3 The impact of empirical calculations

339 In case the underlying emissions and process knowledge is accurate the total modelled deposition using LOTOS-EUROS
340 should be unbiased and thus highly consistent with the assessment results. Hence, deviations between the two provides
341 hints at areas and components that need improvement in the modelling. The latter is important as a CTM is used to explore
342 the effectivity of mitigation strategies. In Figure 8 we present the relative difference between the final assessed total
343 deposition estimates and the modelled total deposition using LOTOS-EUROS. These ratio maps contain the signature of
344 the highly resolved precipitation map as well as the occult deposition on top of a more general distribution. To remove the
345 first structures it is advised to use higher resolved non-hydrostatic meteorological input data as well as to develop a
346 parameterization for occult deposition in the chemistry transport model. The maps also clearly illustrate our finding that
347 the model system underestimates the deposition of oxidized nitrogen. This underestimation is consistent with the air
348 concentrations of nitrogen oxides. Moreover, this finding is consistent with a recent trend study showing that the oxidized
349 nitrogen components are increasingly underestimated over time since 1995 (Banzhaf et al., 2015). In contrast, our model
350 results for reduced nitrogen do not show indications for a large systematic difference as evidenced for large parts of western
351 and central Germany. Only in the east towards the Polish border there are indications that the wet deposition is
352 underestimated. In the southern half of Bavaria the model overestimates the wet deposition of ammonium and the
353 assessment shows a lower total flux by about 20 %. This exceptional behaviour should be explained and we advise to
354 investigate the emission variability as well as the precipitation statistics in more detail.

355

356 3.4 Comparison to previous studies

357 At first we compare our results previously derived nationwide deposition maps obtained for 2007 in the MAPESI project
358 (Bultjes et al., 2011). In principle, in MAPESI the same overall approach was taken as in this study. In comparison to
359 MAPESI the current assessment of total deposition across Germany is lower by 27% (see Table 6). This difference is largely
360 determined by two methodological development steps. Firstly, wet deposition QAQC criteria are more strict in this study



361 and the geostatistical interpolation was improved from ordinary kriging to residual kriging resulting in a 13 % lower total
362 deposition flux than in MAPESI (Wichink Kruit et al., 2014). Secondly, a series of model developments were consolidated
363 in the LOTOS-EUROS version (Banzhaf et al., 2016) The most relevant improvements were the introduction of the
364 compensation point for ammonia following Wichink Kruit et al. (2012), the update of the parameterization for the dry
365 deposition aerosols following Zhang (2001) and the introduction of a new wet deposition parameterization for below and
366 in-cloud scavenging following Banzhaf et al. (2012) which accounts for droplet saturation. Whereas the inclusion of these
367 changes hardly affects the modelled total deposition, the new process descriptions reduced the dry deposition efficiency
368 and led to increased wet deposition fluxes for Germany on average. The shift from dry to wet deposition reduced the bias
369 between modelled and observed wet deposition fluxes considerably, especially for reduced nitrogen. As the empirical
370 derived wet deposition maps replace the model results, this shift impacts the resulting assessment of the total deposition
371 across Germany. The newly modelled wet deposition fluxes by LOTOS-EUROS are closer to observations compared to
372 MAPESI which yields a smaller correction for the wet deposition and thus a lower total deposition estimate. Note that
373 within Germany the update of the model parameterizations also causes redistribution from source areas towards natural
374 areas leading to a smaller decline in the assessed total deposition compared to MAPESI in the large forest areas in Germany.
375 Hence, the reduction in comparison to MAPESI is not a homogeneous reduction across the German territory.

376 In Table 6 also the results of this study are compared to those of EMEP for 2009 as calculated with the emission reporting
377 of 2014 (www.emep.int). Our total N deposition is very close to EMEP results, with a difference of about 6%. Altogether,
378 the comparison between the best estimated reduced N deposition in PINETI-2 and the reported total N deposition by EMEP
379 is good. The spatial distributions of the NO_y and NH_x deposition in the EMEP model are rather similar to ours, although
380 it is obvious that the distributions obtained here show much more structure than the EMEP results due to the higher
381 resolution modelling and high resolution precipitation distribution used here. With respect to oxidized nitrogen the final
382 results for this study are slightly lower than the EMEP model results. However, the LOTOS-EUROS results are significantly
383 lower than the results by EMEP, which is exclusively due to a difference in the wet deposition numbers of both models as
384 the average dry deposition fluxes are almost the same. The systematic underestimation of oxidized nitrogen in precipitation
385 from LOTOS-EUROS is currently under investigation.

386 To evaluate the total nitrogen deposition one relies on scientific studies that measure wet and dry deposition at a single site.
387 In Table 7 the N deposition results are compared with the estimates at few research sites in Germany. Forellenbach is an
388 integrated monitoring site and is located in the Southeast of Germany in the Bavarian forest. Neuglobsow is also an
389 integrated monitoring site and is located in the Northeast of Germany. Bourtangier Moor is a Nature2000 area that is located
390 in the Northwest of Germany, close to the border with the Netherlands. Note that the total N deposition at these stations
391 was determined using different methodologies. For Forellenbach and Neuglobsow our estimates are 20 % higher than
392 estimated based on the local observations. At Bourtangier Moor, a variety of methods to determine total N deposition was
393 explored at different locations in the nature area and a large range of total N deposition estimates was found, i.e., values
394 were in a range from roughly 16 till 35 kg ha⁻¹ yr⁻¹ (Mohr, 2013). Our results for Bourtangier Moor using semi-natural
395 vegetation is 20 Kg N ha⁻¹ yr⁻¹, which is within the observed range although slightly lower than the average of all
396 observations of 25 Kg N ha⁻¹ yr⁻¹. Overall, these comparisons show differences within the anticipated uncertainty as
397 discussed above. Unfortunately, the number of intensive monitoring stations is rather low, which highlights the need for
398 additional locations where dry deposition fluxes are determined.

399 **3.5 Critical loads exceedance**

400 The Critical Load concept delivers effect-based thresholds for the maximum acceptable nitrogen deposition. We compared
401 the established deposition flux for the year 2009 to the Critical Load dataset of Germany for eutrophication (Posch et al.,
402 2012). Regions with rather dry conditions and/or poor sandy soils appear as rather sensitive to nitrogen deposition. About
403 70% of the receptor area is still at risk in the year 2009 for eutrophication due to nutrient nitrogen deposition (see Figure
404 9). About half of the receptor area has values up to $10 \text{ kg ha}^{-1} \text{ a}^{-1}$ nutrient nitrogen, whereas 20 % shows even larger
405 exceedances. Highest exceedances are found for Lower Saxony, Schleswig Holstein, North-Rhein-Westphalia, Saxony and
406 northern Bavaria. It has to be pointed out, that the critical loads and their exceedances shown here are grid average values
407 for a grid size of 1 km^2 and thus valuable for a national assessment of eutrophication or acidification only, but do not serve
408 for local assessments. One has to bear in mind that for a certain location the recommended critical loads for such small
409 scale or vegetation type specific assessments can differ substantially from the critical loads shown here.

410 **4 Conclusions**

411 In this study we have presented the methodology to assess the deposition of reactive nitrogen to ecosystems across
412 Germany. The methodology combines prognostic and empirical modelling to establish land use dependent dry and occult
413 and wet deposition fluxes. On average, the nitrogen in Germany is estimated to be $1057 \text{ eq ha}^{-1} \text{ yr}^{-1}$. Almost two thirds
414 (64%) of the nitrogen deposition is explained by reduced nitrogen. Separate maps are available for the major land use
415 classes. These maps show considerable variability across the German territory with highest deposition on forest ecosystems
416 in or near the main agricultural and industrial areas. The results of this study are systematically lower than provided in
417 earlier national studies, but show a better agreement with results obtained by integrated monitoring and deposition mapping
418 by EMEP. Through comparison of the new deposition distributions with critical load maps it is estimated that 70 % of the
419 ecosystems across Germany receive too much nitrogen.

420 **References**

- 421 Banzhaf, S., Schaap, M., Kerschbaumer, A., Reimer, E., Stern, R., van der Swaluw, E. and Bultjes, P.: Implementation
422 and evaluation of pH-dependent cloud chemistry and wet deposition in the chemical transport model REM-Calgrid, *Atmos.*
423 *Environ.*, 49, 378–390, doi:10.1016/j.atmosenv.2011.10.069, 2012.
- 424 Banzhaf, S., Schaap, M., Kranenburg, R., Manders, A. M. M., Segers, A. J., Visschedijk, A. J. H., Denier van der Gon, H.
425 A. C., Kuenen, J. J. P., van Meijgaard, E., van Ulft, L. H., Cofala, J. and Bultjes, P. J. H.: Dynamic model evaluation for
426 secondary inorganic aerosol and its precursors over Europe between 1990 and 2009, *Geosci. Model Dev.*, 8(4), 1047–1070,
427 doi:10.5194/gmd-8-1047-2015, 2015.
- 428 Banzhaf, S., Schaap, M., Wichink Kruit, R., Kranenburg, R., Manders, A. M. M. and Hendriks, C.: Sensitivity of Modelled
429 Land Use Specific Nitrogen Deposition Fluxes to Improved Process Descriptions., in *Air Pollution Modeling and its*
430 *Application XXIV.*, edited by D. Steyn and N. Chaumerliac, Springer., 2016.
- 431 Beltman, J. B., Hendriks, C., Tum, M. and Schaap, M.: The impact of large scale biomass production on ozone air pollution
432 in Europe, *Atmos. Environ.*, 71, 352–363, doi:10.1016/j.atmosenv.2013.02.019, 2013.
- 433 Blackwell, B. D. and Driscoll, C. T.: Deposition of mercury in forests along a montane elevation gradient, *Environ. Sci.*
434 *Technol.*, 49(9), doi:10.1021/es505928w, 2015.



- 435 Bobbink, R., Hornung, M. and Roelofs, J. G. M.: The effects of air-borne nitrogen pollutants on species diversity in natural
436 and semi-natural European vegetation, *J. Ecol.*, 86, 717–738, doi:DOI 10.1046/j.1365-2745.1998.8650717.x, 1998.
- 437 Bouwman, A. F., Lee, D. S., Asman, W. A. H., Dentener, F. J., Van Der Hoek, K. W. and Olivier, J. G. J.: A global high-
438 resolution emission inventory for ammonia, *Global Biogeochem. Cycles*, 11(4), 561–587, doi:10.1029/97GB02266, 1997.
- 439 Builtjes, P., Hendriks, E., Koenen, M., Schaap, M., Banzhaf, S., Kerschbaumer, A., Gauger, T., Nagel, H.-D., Scheuschner,
440 T. and von Schlutow, A.: Erfassung, Prognose und Bewertung von Stoffeinträgen und ihren Wirkungen in Deutschland
441 (in German). MAPESI-Project: Modeling of Air Pollutants and Ecosystem Impact, Dessau., 2011.
- 442 Crutzen, P. J.: The role of NO and NO₂ in the chemistry of the troposphere and stratosphere., *Annu. Rev. earth Planet. Sci.*
443 Vol. 7, 443–472 [online] Available from: [http://www.scopus.com/inward/record.url?eid=2-s2.0-](http://www.scopus.com/inward/record.url?eid=2-s2.0-0018696028&partnerID=tZOtx3y1)
444 0018696028&partnerID=tZOtx3y1, 1979.
- 445 Curier, R. L., Timmermans, R., Calabretta-Jongen, S., Eskes, H., Segers, A., Swart, D. and Schaap, M.: Improving ozone
446 forecasts over Europe by synergistic use of the LOTOS-EUROS chemical transport model and in-situ measurements,
447 *Atmos. Environ.*, 60, 217–226, doi:10.1016/j.atmosenv.2012.06.017, 2012.
- 448 Curier, R. L., Kranenburg, R., Segers, A. J. S., Timmermans, R. M. A. and Schaap, M.: Synergistic use of OMI NO₂
449 tropospheric columns and LOTOS-EUROS to evaluate the NO_x emission trends across Europe, *Remote Sens. Environ.*,
450 149, 58–69, doi:10.1016/j.rse.2014.03.032, 2014.
- 451 Damgaard, C., Jensen, L., Frohn, L. M., Borchsenius, F., Nielsen, K. E., Ejrnæs, R. and Stevens, C. J.: The effect of nitrogen
452 deposition on the species richness of acid grasslands in Denmark: A comparison with a study performed on a European
453 scale, *Environ. Pollut.*, 159(7), doi:10.1016/j.envpol.2011.04.003, 2011.
- 454 Erisman, J. W. and Schaap, M.: The need for ammonia abatement with respect to secondary PM reductions in Europe,
455 *Environ. Pollut.*, 129(1), 159–163, doi:10.1016/j.envpol.2003.08.042, 2004.
- 456 Erisman, J. W., Möls, H., Fonteijn, P., Geusebroek, M., Draaijers, G., Bleeker, A. and Van Der Veen, D.: Field
457 intercomparison of precipitation measurements performed within the framework of the Pan European Intensive Monitoring
458 Program of EU/ICP Forest, *Environ. Pollut.*, 125(2), doi:10.1016/S0269-7491(03)00082-4, 2003.
- 459 Erisman, J. W., Bleeker, a., Galloway, J. and Sutton, M. S.: Reduced nitrogen in ecology and the environment, *Environ.*
460 *Pollut.*, 150(1), 140–149, doi:10.1016/j.envpol.2007.06.033, 2007.
- 461 Erisman, J. W., Galloway, J., Seitzinger, S., Bleeker, A. and Butterbach-Bahl, K.: Reactive nitrogen in the environment
462 and its effect on climate change, *Curr. Opin. Environ. Sustain.*, 3(5), 281–290, doi:10.1016/j.cosust.2011.08.012, 2011.
- 463 Fountoukis, C. and Nenes, A.: ISORROPIAII: A computationally efficient thermodynamic equilibrium model for K+-
464 Ca²⁺-Mg²⁺-NH₄⁺-Na⁺-SO₄²⁻-NO₃⁻-Cl⁻-H₂O aerosols, *Atmos. Chem. Phys.*, 7(17), 2007.
- 465 Fowler, D., Pilegaard, K., Sutton, M. a., Ambus, P., Raivonen, M., Duyzer, J., Simpson, D., Fagerli, H., Fuzzi, S.,
466 Schjoerring, J. K., Granier, C., Neftel, a., Isaksen, I. S. a, Laj, P., Maione, M., Monks, P. S., Burkhardt, J., Daemmgen, U.,
467 Neiryneck, J., Personne, E., Wichink-Kruit, R., Butterbach-Bahl, K., Flechard, C., Tuovinen, J. P., Coyle, M., Gerosa, G.,
468 Loubet, B., Altimir, N., Gruenhage, L., Ammann, C., Cieslik, S., Paoletti, E., Mikkelsen, T. N., Ro-Poulsen, H., Cellier, P.,
469 Cape, J. N., Horváth, L., Loreto, F., Niinemets, Ü., Palmer, P. I., Rinne, J., Misztal, P., Nemitz, E., Nilsson, D., Pryor, S.,



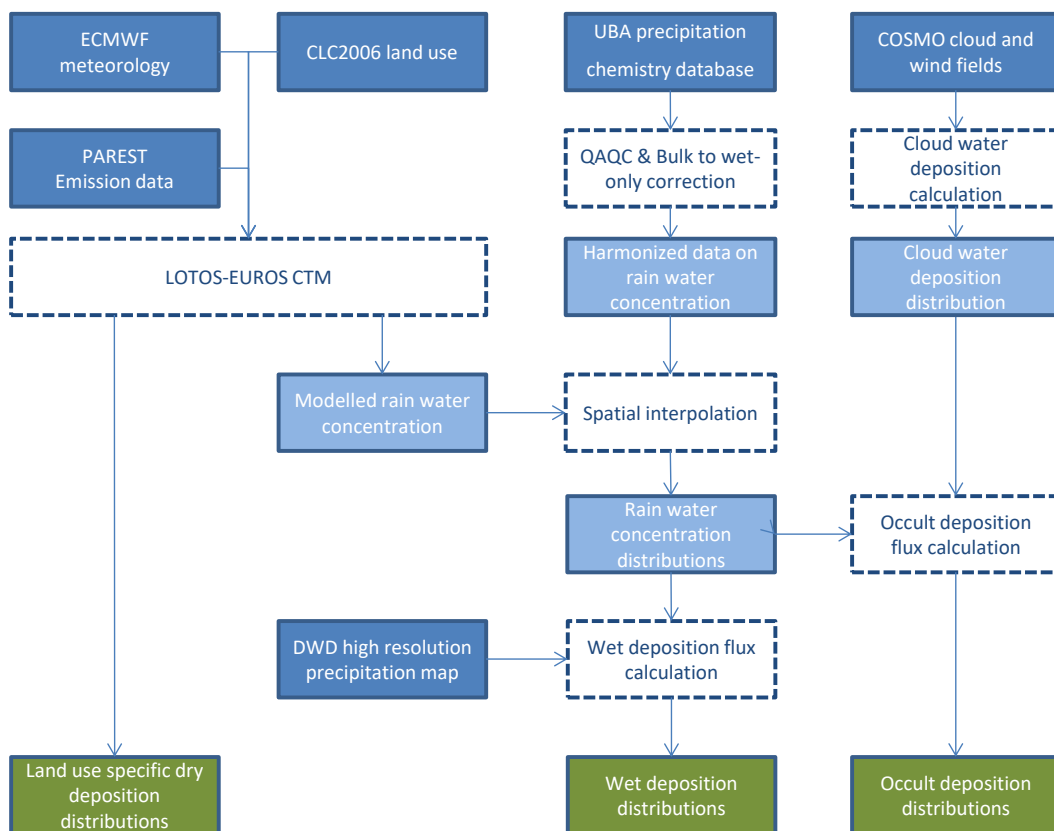
- 470 Gallagher, M. W., Vesala, T., Skiba, U., Brüggemann, N., Zechmeister-Boltenstern, S., Williams, J., O'Dowd, C., Facchini,
471 M. C., de Leeuw, G., Flossman, a., Chaumerliac, N. and Erisman, J. W.: Atmospheric composition change: Ecosystems-
472 Atmosphere interactions, *Atmos. Environ.*, 43(33), 5193–5267, doi:10.1016/j.atmosenv.2009.07.068, 2009.
- 473 Fowler, D., Pyle, J. a, Raven, J. a, Sutton, M. a and B, P. T. R. S.: The global nitrogen cycle in the twenty-first century :
474 introduction The global nitrogen cycle in the twenty- first century : introduction, , (May), 2013–2015, 2013.
- 475 Galloway, J. N., Aber, J. D., Erisman, J. W., Seitzinger, S. P., Howarth, R. W., Cowling, E. B. and Cosby, B. J.: The
476 Nitrogen Cascade, *Bioscience*, 53(4), 341, doi:10.1641/0006-3568(2003)053[0341:TNC]2.0.CO;2, 2003.
- 477 Gauger, T., Haenel, H., Rösemann, C., Ulrich, D., Bleeker, A., Erisman, J., Vermeulen, A., Schaap, M., Timmermanns, R.,
478 Builtjes, P. and Duyzer, J.: National Implementation of the UNECE Convention on Long-range Transboundary Air
479 Pollution (Effects) / Nationale Umsetzung UNECELuftreinhaltekonvention (Wirkungen): Part 1: Deposition Loads:
480 Methods, modelling and mapping results, trends., Dessau., 2008.
- 481 Geupel, M. and Frommer, J.: Reactive Nitrogen in Germany - Causes and effects - measures and recommendations.,
482 Dessau., 2015.
- 483 Grubbs, F.: Procedures for Detecting Outlying Observations in Samples, *Technometrics*, 11, 1–21, 1969.
- 484 Hendriks, C., Kranenburg, R., Kuenen, J., van Gijlswijk, R., Wichink Kruit, R., Segers, A., Denier van der Gon, H. and
485 Schaap, M.: The origin of ambient particulate matter concentrations in the Netherlands, *Atmos. Environ.*, 69, 289–303,
486 doi:10.1016/j.atmosenv.2012.12.017, 2013.
- 487 Hendriks, C., Kranenburg, R., Kuenen, J. J. P., Van den Bril, B., Verguts, V. and Schaap, M.: Ammonia emission time
488 profiles based on manure transport data improve ammonia modelling across north western Europe, *Atmos. Environ.*, 131,
489 83–96, doi:10.1016/j.atmosenv.2016.01.043, 2016.
- 490 Hertel, O., Skjøth, C. a., Reis, S., Bleeker, a., Harrison, R., Cape, J. N., Fowler, D., Skiba, U., Simpson, D., Jickells, T.,
491 Kulmala, M., Gylldenkerne, S., Sørensen, L. L., Erisman, J. W. and Sutton, M. a.: Governing processes for reactive nitrogen
492 compounds in the atmosphere in relation to ecosystem, climatic and human health impacts, *Biogeosciences Discuss.*, 9(7),
493 9349–9423, doi:10.5194/bgd-9-9349-2012, 2012.
- 494 Herzog, J. and Muller-Westermeier, G.: Homogenitätsprüfung und homogenisierung klimatologischer meßreihen im
495 deutschen wetterdienst., *Deutsche Wetterdienst.*, 1998.
- 496 Hettelingh, J.-P., Posch, M., De Smet, P. A. M. and Downing, R. J.: The use of critical loads in emission reduction
497 agreements in Europe, *Water, Air, & Soil Pollut.*, 85(4), doi:10.1007/BF01186190, 1995.
- 498 Hettelingh, J.-P., Posch, M., Velders, G. J. M., Ruysenaars, P., Adams, M., de Leeuw, F., Lükewille, A., Maas, R., Sliggers,
499 J. and Slootweg, J.: Assessing interim objectives for acidification, eutrophication and ground-level ozone of the EU
500 National Emission Ceilings Directive with 2001 and 2012 knowledge, *Atmos. Environ.*, 75,
501 doi:10.1016/j.atmosenv.2013.03.060, 2013.
- 502 Jörß, W., Kugler, U. and Theloke, J.: Emissionen im PAREST Referenzszenario 2005-2020, Dessau., 2010.
- 503 Katata, G., Nagai, H., Wrzesinsky, T., Klemm, O., Eugster, W. and Burkard, R.: Development of a land surface model
504 including cloud water deposition on vegetation, *J. Appl. Meteorol. Climatol.*, 47(8), doi:10.1175/2008JAMC1758.1, 2008.



- 505 Katata, G., Kajino, M., Hiraki, T., Aikawa, M., Kobayashi, T. and Nagai, H.: A method for simple and accurate estimation
506 of fog deposition in a mountain forest using a meteorological model, *J. Geophys. Res. Atmos.*, 116(20),
507 doi:10.1029/2010JD015552, 2011.
- 508 Klemm, O. and Wrzesinsky, T.: Fog deposition fluxes of water and ions to a mountainous site in Central Europe, *Tellus*,
509 Ser. B Chem. Phys. Meteorol., 59(4), doi:10.1111/j.1600-0889.2007.00287.x, 2007.
- 510 Kuenen, J. J. P., Visschedijk, A. J. H., Jozwicka, M. and Denier Van Der Gon, H. A. C.: TNO-MACC-II emission inventory;
511 A multi-year (2003-2009) consistent high-resolution European emission inventory for air quality modelling, *Atmos. Chem.*
512 *Phys.*, 14(20), doi:10.5194/acp-14-10963-2014, 2014.
- 513 Manders, A. M. M., Schaap, M. and Hoogerbrugge, R.: Testing the capability of the chemistry transport model LOTOS-
514 EUROS to forecast PM10 levels in the Netherlands, *Atmos. Environ.*, 43(26), 4050–4059,
515 doi:10.1016/j.atmosenv.2009.05.006, 2009.
- 516 Manders, A. M. M., Schaap, M., Querol, X., Albert, M. F. M. A., Vercauteren, J., Kuhlbusch, T. A. J. and Hoogerbrugge,
517 R.: Sea salt concentrations across the European continent, *Atmos. Environ.*, 44(20), 2434–2442,
518 doi:10.1016/j.atmosenv.2010.03.028, 2010.
- 519 Mohr, C.: Emsland: Erfassung der Stickstoffbelastungen aus der Tierhaltung zur Erarbeitung innovativer Lösungsansätze
520 für eine zukunftsfähige Landwirtschaft bei gleichzeitigem Schutz der sensiblen Moorlandschaft (ERNST), Emsland., 2013.
- 521 Posch, M., Slootweg, J. and Hettelingh, J.-P.: Modelling and Mapping of Atmospherically-induced Ecosystem Impacts in
522 Europe., 2012.
- 523 Rihm, B. and Kurz, D.: Deposition and critical loads of nitrogen in Switzerland, *Water. Air. Soil Pollut.*, 130(1–4 III),
524 doi:10.1023/A:1013972915946, 2001.
- 525 Schaap, M., van Loon, M., ten Brink, H. M., Dentener, F. J. and Bultjes, P. J. H.: Secondary inorganic aerosol simulations
526 for Europe with special attention to nitrate, *Atmos. Chem. Phys.*, 4(3), 857–874 [online] Available from:
527 <http://www.scopus.com/inward/record.url?eid=2-s2.0-3242875516&partnerID=tZOtx3y1>, 2004.
- 528 Schaap, M., Timmermans, R. M. A., Roemer, M., Boersen, G. A. C., Bultjes, P. J. H., Sauter, F. J., Velders, G. J. M. and
529 Beck, J. P.: The LOTOS EUROS model: description, validation and latest developments, *Int. J. Environ. Pollut.*, 32(2),
530 270, doi:10.1504/IJEP.2008.017106, 2008.
- 531 Schaap, M., Otjes, R. P. and Weijers, E. P.: Illustrating the benefit of using hourly monitoring data on secondary inorganic
532 aerosol and its precursors for model evaluation, *Atmos. Chem. Phys.*, 11(21), 11041–11053, doi:10.5194/acp-11-11041-
533 2011, 2011.
- 534 Schaap, M., Kranenburg, R., Curier, L., Jozwicka, M., Dammers, E. and Timmermans, R.: Assessing the Sensitivity of the
535 OMI-NO2 Product to Emission Changes across Europe, *Remote Sens.*, 5(9), 4187–4208, doi:10.3390/rs5094187, 2013.
- 536 Schrader, F. and Brümmer, C.: Genfer Luftreinhaltekonvention der UNECE: Literaturstudie zu Messungen der Ammoniak-
537 Depositionsgeschwindigkeit, UBA-Texte, (67/2014), 2014.
- 538 Simpson, D., Butterbach-Bahl, K., Fagerli, H., Kesik, M., Skiba, U. and Tang, S.: Deposition and emissions of reactive
539 nitrogen over European forests: A modelling study, *Atmos. Environ.*, 40(29), doi:10.1016/j.atmosenv.2006.04.063, 2006.



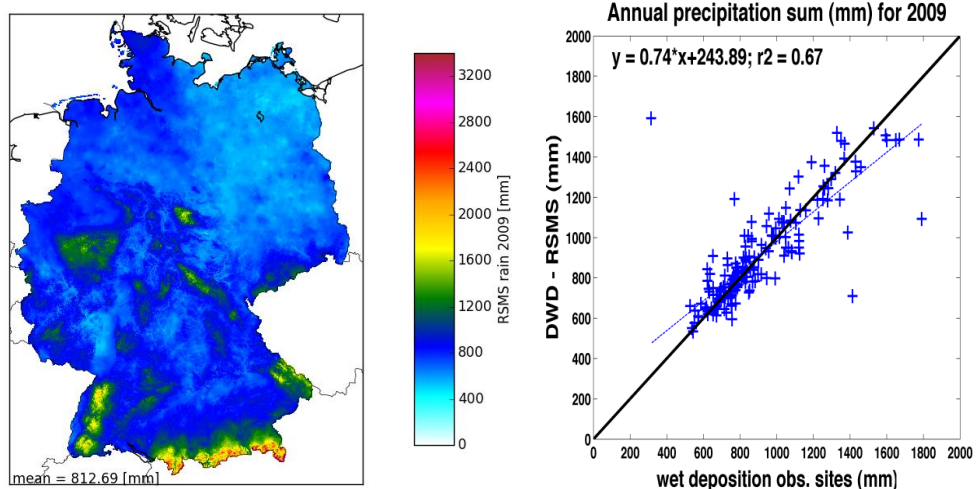
- 540 Simpson, D., Benedictow, A., Berge, H., Bergström, R., Emberson, L. D., Fagerli, H., Flechard, C. R., Hayman, G. D.,
541 Gauss, M., Jonson, J. E., Jenkin, M. E., Nyíri, A., Richter, C., Semeena, V. S., Tsyro, S., Tuovinen, J.-P., Valdebenito, A.
542 and Wind, P.: The EMEP MSC-W chemical transport model – Technical description, *Atmos. Chem. Phys.*,
543 12(16), doi:10.5194/acp-12-7825-2012, 2012.
- 544 Sutton, M. a, Oenema, O., Erisman, J. W., Leip, A., van Grinsven, H. and Winiwarter, W.: Too much of a good thing.,
545 *Nature*, 472(7342), 159–161, doi:10.1038/472159a, 2011.
- 546 Tørseth, K., Aas, W., Breivik, K., Fjæraa, A. M., Fiebig, M., Hjellbrekke, A. G., Lund Myhre, C., Solberg, S. and Yttri, K.
547 E.: Introduction to the European Monitoring and Evaluation Programme (EMEP) and observed atmospheric composition
548 change during 1972–2009, *Atmos. Chem. Phys.*, 12(12), doi:10.5194/acp-12-5447-2012, 2012.
- 549 Van Damme, M., Wichink Kruit, R. J., Schaap, M., Clarisse, L., Clerbaux, C., Coheur, P.-F., Dammers, E., Dolman, A. J.
550 and Erisman, J. W.: Evaluating 4 years of atmospheric ammonia (NH₃) over Europe using IASI satellite observations and
551 LOTOS-EUROS model results, *J. Geophys. Res. Atmos.*, 119(15), 9549–9566, doi:10.1002/2014JD021911, 2014.
- 552 Vautard, R., Van Loon, M., Schaap, M., Bergström, R., Bessagnet, B., Brandt, J., Builtjes, P. J. H., Christensen, J. H.,
553 Cuvelier, C., Graff, A., Jonson, J. E., Krol, M., Langner, J., Roberts, P., Rouil, L., Stern, R., Tarrasón, L., Thunis, P.,
554 Vignati, E., White, L. and Wind, P.: Is regional air quality model diversity representative of uncertainty for ozone
555 simulation?, *Geophys. Res. Lett.*, 33(24), L24818, doi:10.1029/2006GL027610, 2006.
- 556 Vlemmix, T., Eskes, H. J., Peters, A. J. M., Schaap, M., Sauter, F. J., Kelder, H. and Levelt, P. F.: MAX-DOAS tropospheric
557 nitrogen dioxide column measurements compared with the Lotos-Euros air quality model, *Atmos. Chem. Phys.*, 15(3),
558 1313–1330, doi:10.5194/acp-15-1313-2015, 2015.
- 559 Waldner, P., Marchetto, A., Thimonier, A., Schmitt, M., Rogora, M., Granke, O., Mues, V., Hansen, K., Pihl Karlsson, G.,
560 Žlindra, D., Clarke, N., Verstraeten, A., Lazdins, A., Schimming, C., Iacoban, C., Lindroos, A.-J., Vangelova, E., Benham,
561 S., Meesenburg, H., Nicolas, M., Kowalska, A., Apuhtin, V., Napa, U., Lachmanová, Z., Kristoefel, F., Bleeker, A.,
562 Ingerslev, M., Vesterdal, L., Molina, J., Fischer, U., Seidling, W., Jonard, M., O’Dea, P., Johnson, J., Fischer, R. and
563 Lorenz, M.: Detection of temporal trends in atmospheric deposition of inorganic nitrogen and sulphate to forests in Europe,
564 *Atmos. Environ.*, 95, doi:10.1016/j.atmosenv.2014.06.054, 2014.
- 565 Wichink Kruit, R., Schaap, M., Segers, A., Banzhaf, S., Scheuschner, T., Builtjes, P. and Heslinga, D.: PINETI (Pollutant
566 INput and EcosysTem Impact) report. Modelling and mapping of atmospheric nitrogen and sulphur deposition and critical
567 loads for ecosystem specific assessment of threats to biodiversity in Germany, Dessau., 2014.
- 568 Wichink Kruit, R. J., Schaap, M., Sauter, F. J., van Zanten, M. C. and van Pul, W. A. J.: Modeling the distribution of
569 ammonia across Europe including bi-directional surface–atmosphere exchange, *Biogeosciences*, 9(12), 5261–5277,
570 doi:10.5194/bg-9-5261-2012, 2012.
- 571 Van Zanten, M., Sauter, F., Wichink Kruit, R., Van Jaarsveld, J. and Van Pul, A.: Description of the DEPAC module: Dry
572 deposition modelling with DEPAC, Bilthoven., 2010.
- 573 Zhang, L., Gong, S., Padro, J. and Barrie, L.: A size-segregated particle dry deposition scheme for an atmospheric aerosol
574 module, *Atmos. Environ.*, 35(3), doi:10.1016/S1352-2310(00)00326-5, 2001.
- 575



576

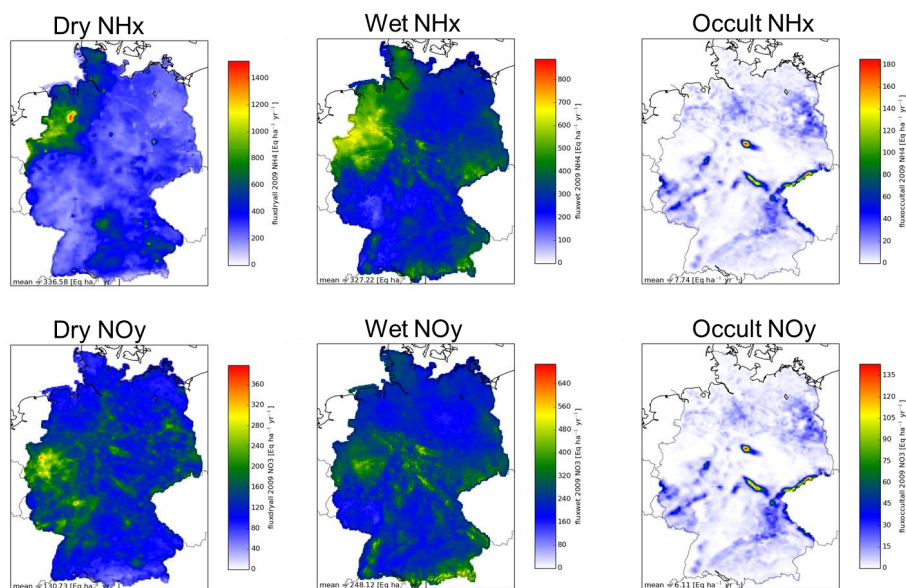
577 **Figure 1. Overview of the assessment methodology used in this study. The scheme introduces important input data**
 578 **(dark blue boxes), key intermediate results (light blue boxes), calculation steps (dashed boxes) and final results**
 579 **(green boxes). The arrows indicate the data flow and dependencies.**

580



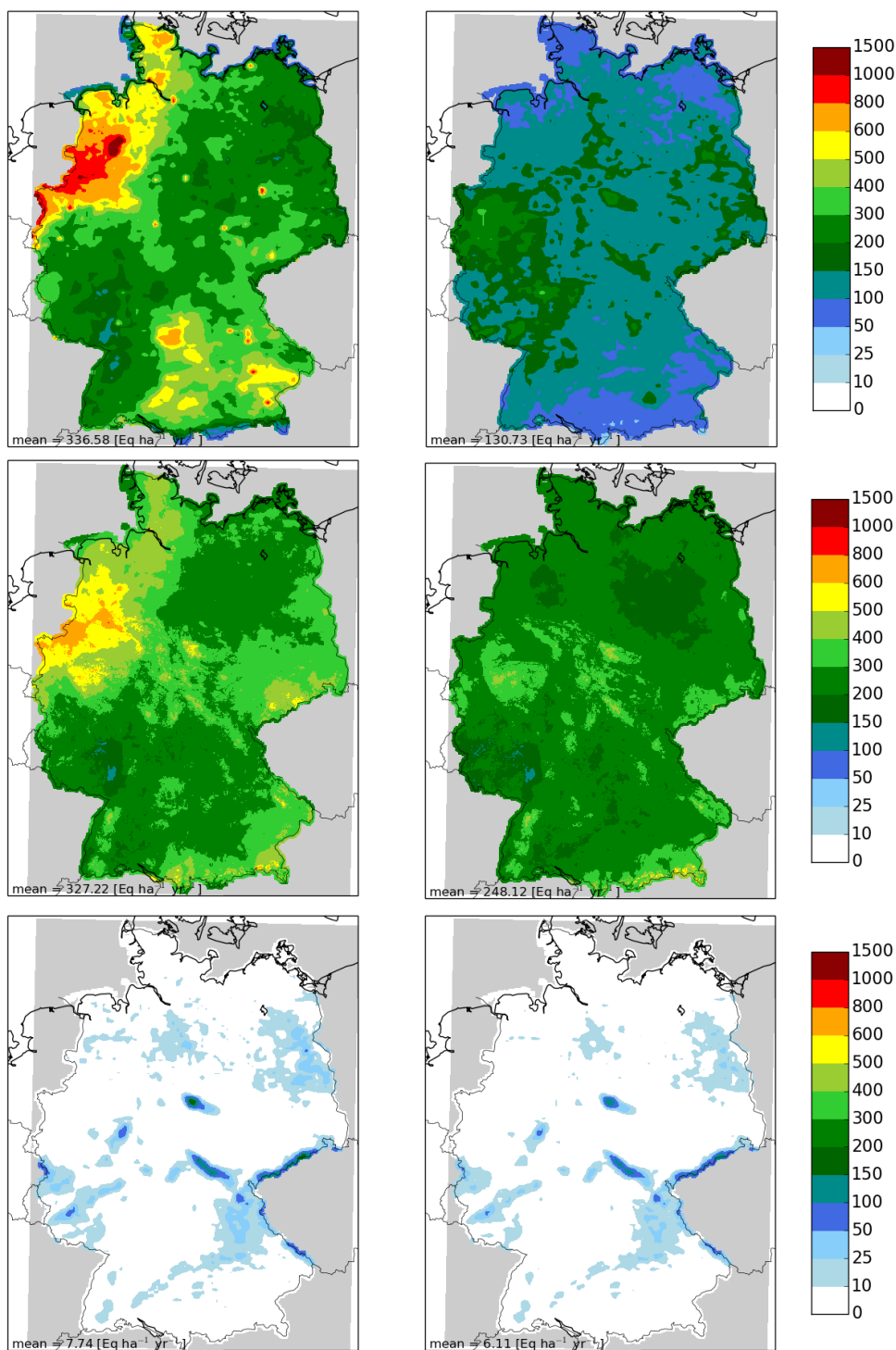
581
 582
 583
 584

Figure 2. High resolution precipitation map (left) and its validation against the independent data from the stations with precipitation chemistry



585
 586
 587
 588

Figure 3. Annual distributions of dry (left), wet (middle) and occult (right) deposition flux ($\text{eq ha}^{-1} \text{a}^{-1}$) for reduced (top) and oxidized (bottom) nitrogen for 2009.

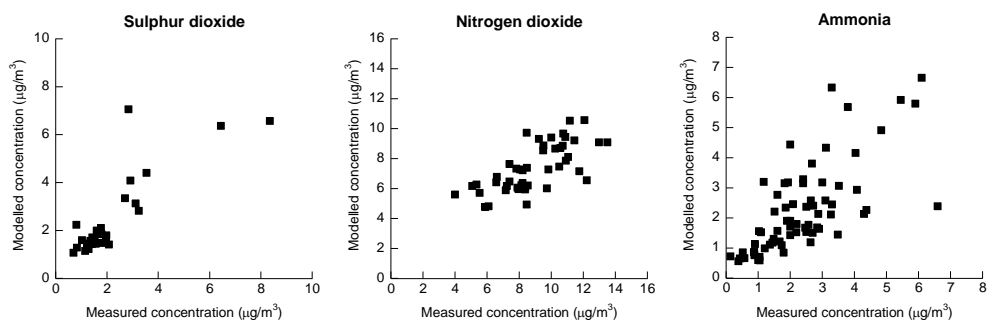


589

Figure 4. Annual distributions of dry (top), wet (middle) and occult (bottom) deposition flux (eq ha⁻¹ a⁻¹) for reduced (left) and oxidized (right) nitrogen for 2009.

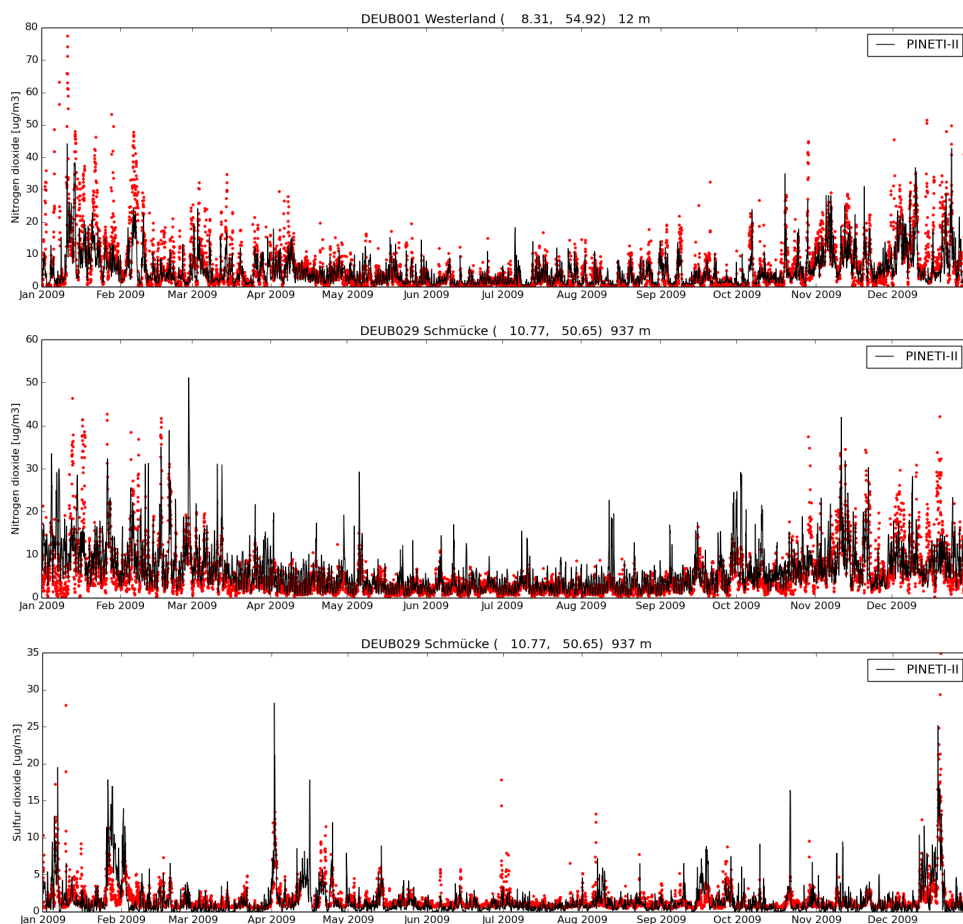


590



591

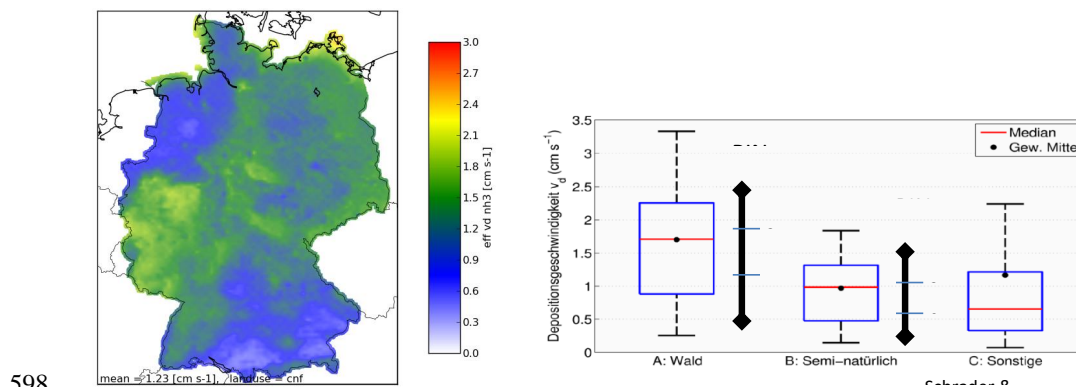
592 **Figure 5. Comparison between modelled and measured annual mean concentrations ($\mu\text{g}/\text{m}^3$) of sulfur dioxide, nitrogen dioxide**
593 **and ammonia at stations across Germany**



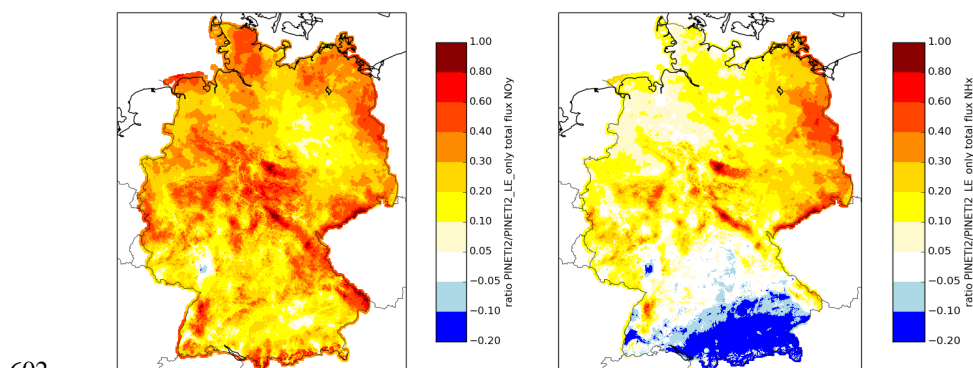
594



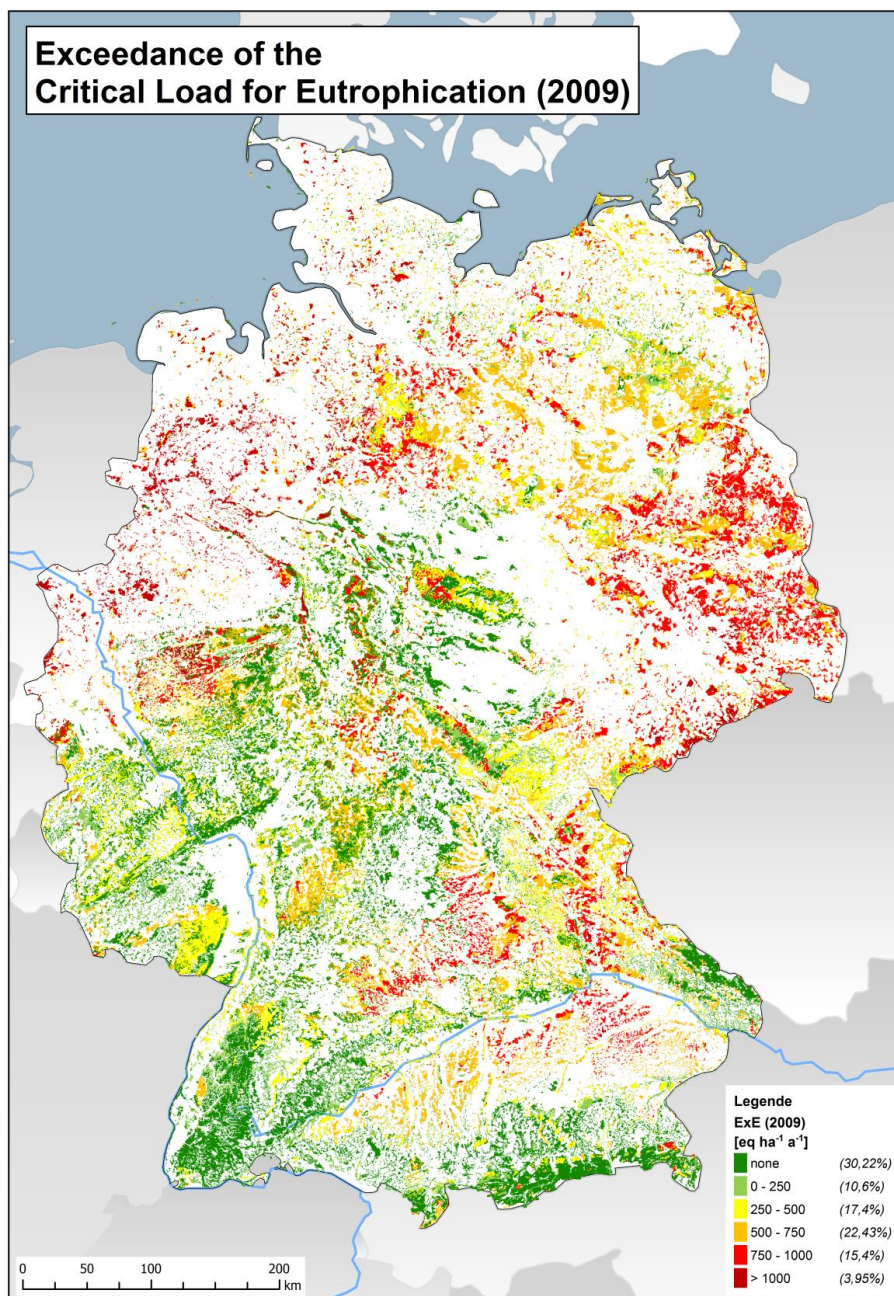
595 **Figure 6. Comparison between measured and modelled concentration ($\mu\text{g}/\text{m}^3$) time series for NO_2 and SO_2 at the UBA stations**
 596 **Westerland and Schmücke.**
 597



598
 599 **Figure 7. Dry deposition velocity above coniferous forest (left) and a comparison between the range of annual mean dry deposition**
 600 **velocities for ammonia across Germany and the range average of ammonia deposition velocities reported in literature (Schrader**
 601 **and Brümmer, 2014).**



602
 603 **Figure 8. Relative difference ((Assessment – LOTOSEUROS) / Assessment) of the total deposition of NO_y (left) and NH_x (right)**
 604 **between the modelled distributions and the final assessment including empirical wet and occult deposition estimates.**



605

606

Figure 9. Critical load exceedance for reactive nitrogen deposition across Germany

607



609 **Table 1. Enrichment factors for occult deposition as used in this study.**

<i>Species</i>	<i>Mean enrichment factor</i>
SO ₄ ²⁻	7.0
NO ₃ ⁻	8.6
NH ₄ ⁺	9.2

610 **Table 2. Overview of averaged estimates of dry, wet and total deposition fluxes (eq ha⁻¹ yr⁻¹) per land use category across the**
 611 **German territory for reactive nitrogen. The average over the German territory was obtained using the actual land use**
 612 **distribution**

Land use	<i>Code</i>	<i>N_{tot}</i>	<i>Dry NH_x</i>	<i>Dry NO_y</i>	<i>Wet NH_x</i>	<i>Wet NO_y</i>	<i>Occult NH_x</i>	<i>Occult NO_y</i>
Grassland	grs	901	228	97	327	248	-	-
Semi-natural	sem	948	250	122	327	248	-	-
Arable	ara	982	296	111	327	248	-	-
Permanent crops	crp	1043	330	137	327	248	-	-
Coniferous forest	cnf	1287	485	182	327	248	26	19
Deciduous forest	dec	1183	397	162	327	248	28	21
Mixed forest	mix	1235	441	172	327	248	27	20
Water	wat	861	221	64	327	248	-	-
Urban	urb	1248	501	172	327	248	-	-
Other	oth	894	239	80	327	248	-	-
Germany	DEU	1057	337	131	327	248	8	6

613

614 **Table 3. Summary of the statistical model evaluation for SO₂ and NO₂. The data represent the averages over all N stations. We**
 615 **present the observed and modelled mean concentration as well as the variability expressed as a standard deviation (STD).**
 616 **Furthermore, the bias, root mean squared error (RMSE) and temporal correlation coefficient (COR) are given. The evaluation**
 617 **was performed with time series of daily means.**

	N	MEAN_{OBS}	MEAN_{MOD}	STD_{OBS}	STD_{MOD}	BIAS	RMSE	R²
SO₂	31	2.1	2.4	2.0	2.3	0.26	2.2	0.59
NO₂	45	9.0	7.4	6.5	4.8	-1.5	5.1	0.71

618

619 **Table 4. Land use dependent annual effective and average dry deposition velocity at 2.5 meter height (above zero-displacement**
 620 **height and roughness length) across land use types in Germany for six components in cm/s.**

Vd	NO₂		NO		HNO₃		NH₃		SO₂		NH₄²⁻ (fine)	
	Eff	Ave	Eff	Ave	Eff	Ave	Eff	Ave	Eff	Ave	Eff	Ave
ara	0.10	0.15	0.03	0.02	1.20	1.04	0.71	0.82	0.32	0.46	0.08	0.09
cnf	0.15	0.24	0.03	0.02	1.63	1.52	1.23	1.83	0.75	0.91	0.16	0.20



dec	0.13	0.21	0.03	0.02	1.63	1.52	0.95	1.48	0.74	0.90	0.16	0.20
grs	0.08	0.15	0.03	0.02	1.11	0.98	0.58	0.88	0.56	0.63	0.07	0.08
oth	0.07	0.07	0.05	0.05	0.89	0.81	0.56	0.56	0.21	0.30	0.04	0.04
crp	0.13	0.18	0.03	0.02	1.42	1.22	0.81	1.03	0.66	0.76	0.10	0.11
sem	0.08	0.16	0.03	0.02	1.24	1.08	0.63	0.97	0.60	0.68	0.10	0.12
wat	0.05	0.05	0.05	0.05	0.67	0.62	0.48	0.60	0.59	0.57	0.08	0.09
urb	0.08	0.08	0.08	0.08	2.94	2.58	1.09	1.32	0.43	0.82	0.14	0.17
mix	0.14	0.23	0.03	0.02	1.63	1.52	1.09	1.65	0.75	0.90	0.16	0.20

621

622 **Table 5. Comparison of wet deposition fluxes (eq ha⁻¹ yr⁻¹) averaged over all available stations for the year 2009. The bias is**
 623 **provide in an absolute and relative sense**

<i>Variable</i>	<i>Observed</i>	<i>Modelled</i>	<i>Bias</i>	<i>Relative bias (%)</i>
NH _x	295	234	-61	-21
NO _y	226	139	-87	-38

624 **Table 6. Comparison of the average total NO_y, NH_x and N deposition for Germany in this study, the LOTOS-EUROS model,**
 625 **EMEP and the previous German assessment MAPESI by Buitjes et al. (2012).**

	<i>This study</i>	<i>LOTOS-EUROS</i>	<i>EMEP</i>	<i>Buitjes et al., 2011</i>
Year	2009	2009	2009	2005
NO _y	385	298	436	548
NH _x	672	612	690	895
total N	1057	910	1126	1443

626

627 **Table 7. Comparison of the mapped total N- deposition results derived in this study and MAPESI (Buitjes et al., 2011) to**
 628 **empirical derived N deposition estimates (Kg N ha⁻¹ a⁻¹) for three sites across Germany: Forellenbach (Beudert and Breit, 2014),**
 629 **Neuglobsow (Schulte-Bisping and Beese, 2016) and Bourtanger Moor (Mohr, 2013).**

630

	<i>Empirical</i>	<i>MAPESI</i>	<i>This study</i>	<i>Ref</i>
Forellenbach	15	37	19	Beudert and Breit, 2014
Neuglobsow	9.5	18	12	Schulte-Bisping and Beese, 2016
Bourtanger Moor	25 (16-35)	38	20	Mohr, 2013

631